



Correction to: Effect of Process Parameters on Defects, Melt Pool Shape, Microstructure, and Tensile Behavior of 316L Stainless Steel Produced by Selective Laser Melting

Hua-Zhen Jiang^{1,2} · Zheng-Yang Li² · Tao Feng³ · Peng-Yue Wu³ · Qi-Sheng Chen^{1,2} · Yun-Long Feng³ · Long-Fei Chen³ · Jing-Yu Hou^{1,2} · He-Jian Xu²

© The Chinese Society for Metals (CSM) and Springer-Verlag GmbH Germany, part of Springer Nature 2020

Correction to: Acta Metallurgica Sinica (English Letters)
<https://doi.org/10.1007/s40195-020-01143-8>

In the Original Publication of the article, some reference numbers in the Figs. 1, 5, 14 and Appendixes B, C, D are mismatched. The corrected reference numbers in the figures and appendixes are given below.

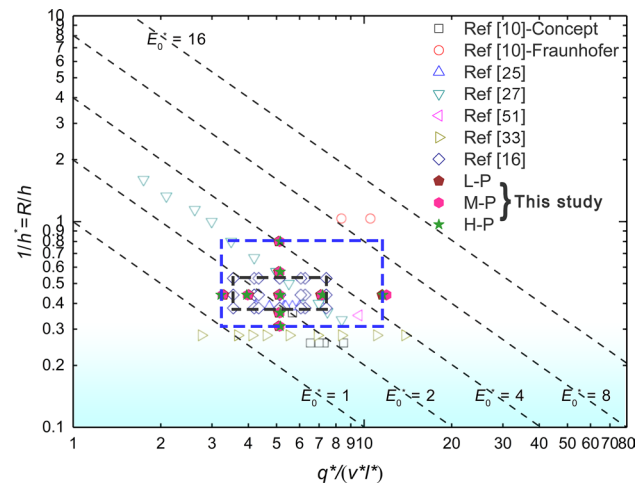


Fig. 1 Normalized process map showing the location of dimensional variables corresponding to the experimental process parameters selected from Table 1. (The experimental data are enclosed in the blue dashed rectangle and the boundary of the experimental data in Ref. [16] is the black dashed rectangle.) Contours of constant normalized equivalent energy density, E_0^* , are provided by the dashed lines

The original article can be found online at <https://doi.org/10.1007/s40195-020-01143-8>.

✉ Zheng-Yang Li
zyli@imech.ac.cn

✉ Qi-Sheng Chen
qschen@imech.ac.cn

¹ School of Engineering Science, University of Chinese Academy of Sciences, Beijing 100190, China

² Institute of Mechanics, Chinese Academy of Sciences, Beijing 100190, China

³ Beijing E-Plus-3D Technology Co., LTD, Beijing 102299, China

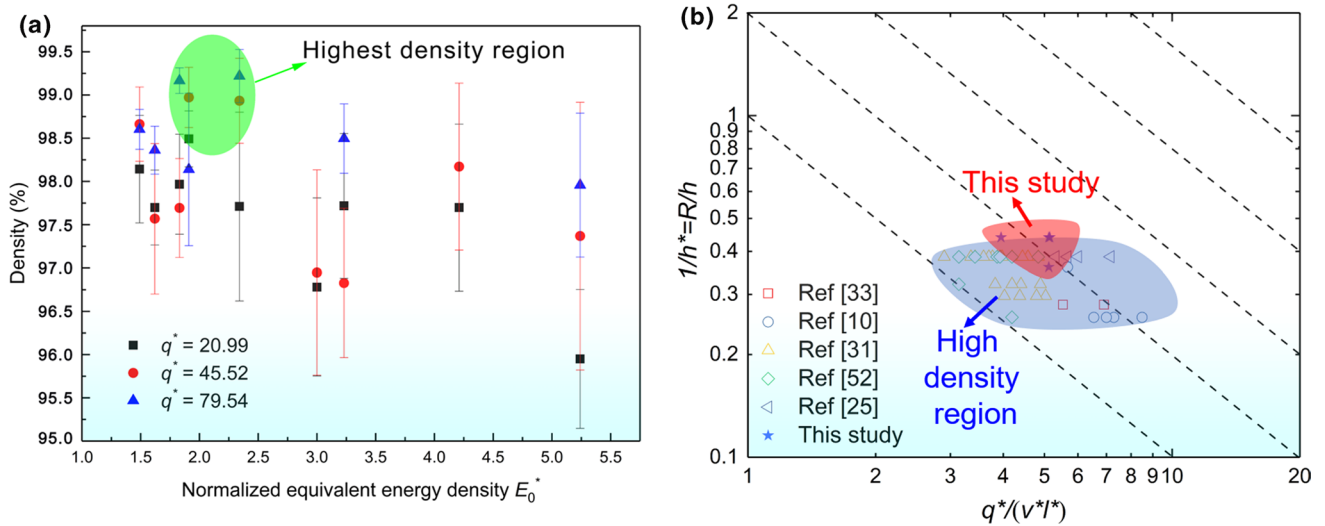


Fig. 5 Effect of process parameters on relative density: **a** density measurement results, **b** a normalized processing diagram showing the location of high-density (> 99%) SLM-processed part. The dashed lines represent contours of constant E_0^*

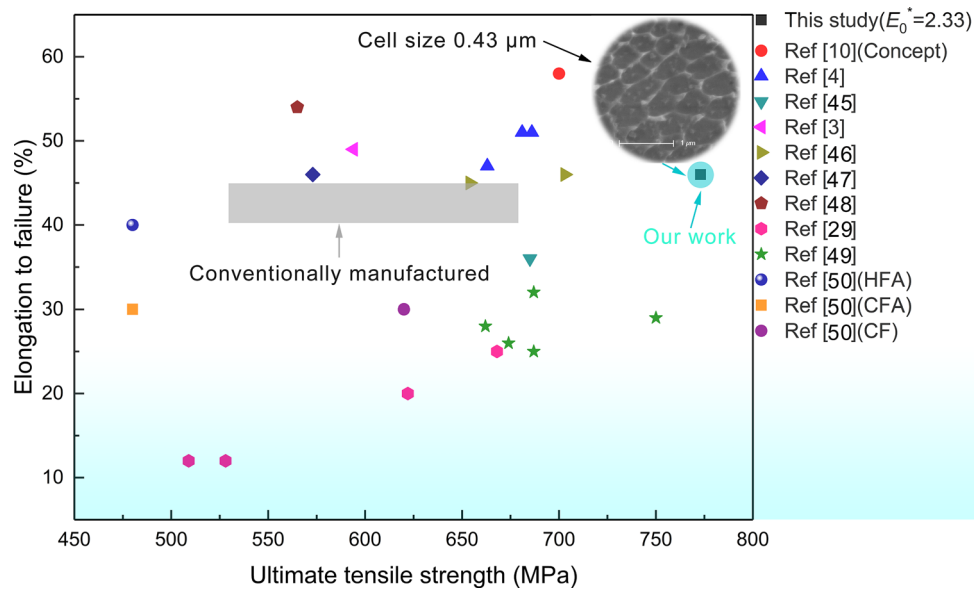
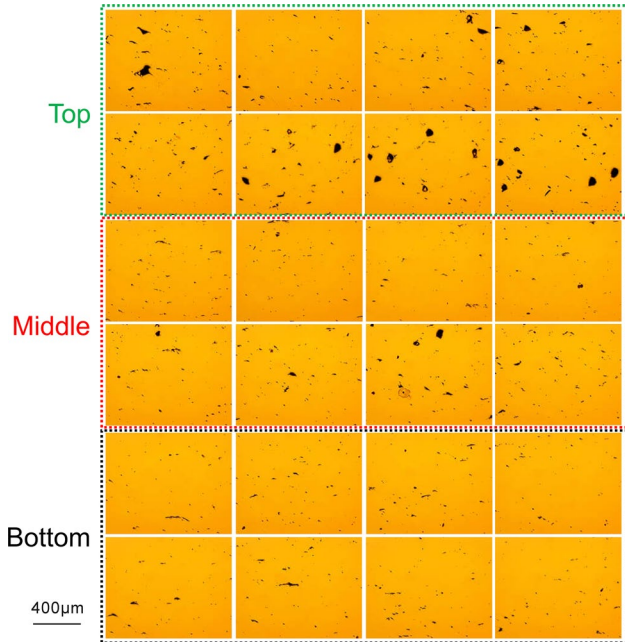


Fig. 14 Summary of ultimate tensile strength versus elongation to failure for 316L SS from our work and previous studies. (The mechanical performance range of conventional wrought 316L SS is shown in the block region; HFA—hot finished + annealed; CFA—cold finished + annealed; CF—cold finished.)

Appendix B

An example of using 24 OM images to examine the relative density of a SLM-manufactured part at a certain process parameter (Sample No. 12)



Sample	YS (MPa)	UTS (MPa)	Uniform elongation (%)	ϵ_f (%)
	456	703	–	46
Liu et al. [11]	552	–	–	83
Sun et al. for 380 W sample [9]	567	660*	–	40*
Wang et al. [39]	–	590	21	–
Elangeswaran et al. [47]	453	573	–	46
Riemer et al. [48]	462	565	–	54
	512	622	–	20
Suryawanshi et al. [29]	430	509	–	12
	536	668	–	25
	449	528	–	12
	517	687	–	32
	463	687	–	25
Kurzynowski et al. [49]	454	750	–	29
	440	662	–	28
	409	674	–	26
Hot finished + annealed [50]	170	480	–	40
Cold finished + annealed [50]	170	480	–	30
Cold finished [50]	310	620	–	30

Appendix C

The maximal temperature rising of a Gaussian beam source exerted on the surface of a substrate is given by Bäuerle [44].

Appendix D

Tensile test results for SLM-processed 316L SS samples are compared with conventionally made samples. The data were extracted from different studies (*—obtained by estimating from tensile engineering stress–strain curves)

Sample	YS (MPa)	UTS (MPa)	Uniform elongation (%)	ϵ_f (%)
This study ($E_0^* = 1.49$)	549 ± 8	708 ± 5	24 ± 3	29 ± 6
This study ($E_0^* = 2.33$)	584 ± 16	773 ± 4	28 ± 1	46 ± 1
Wang et al. [10] (Concept)	595–680	700	34 ± 3	58*
Wang et al. [10] (Fraunhofer)	450–557	640	59	87*
Qiu et al. [4]	558	686	–	51
	541	681	–	51
	519	663	–	47
Casati et al. [45]	554	685	–	36
Zhong et al. [3]	487	594	–	49
Saeidi et al. [46]	428	654	–	45